CIVIL ENGINEERING JOURNAL

Article no. 42

THE CIVIL ENGINEERING JOURNAL 4-2022

AN EXPERIMENTAL STUDY ON SHEAR PERFORMANCE OF ADHESIVE INTERFACE BETWEEN STEEL PLATES AND CFRP

Yi Yang, Qianziyang Zhou, Jiahao Bai and Xinyan Guo

School of Civil Engineering and Transportation, South China University of Technology, Guangzhou 510640, China; liyang01245@126.com

ABSTRACT

CFRP (Carbon Fiber Reinforced Polymer) is widely used in steel structural reinforcement. For steel structures strengthened with CFRPs, except the cases the structures have defects before strengthening, the adhesive interface is the weakest part and CFRP debonding is the most common failure mode. In order to investigate the failure mechanism of CFRP strengthened steel structures, this paper presents an experimental study on shear performance of adhesive interface between CFRPs and steel plates by twin shear model. Six steel plates strengthened with CFRP are divided into two groups, one has no damage, another has a gap at the mid. The specimens are tested under tensile loadings. The experimental results show that, the plates with a gap failed for CFRPs debonding, the cracking loading and breaking loading are 14.85kN, and 17.88kN respectively; the strain-loading curves had long linear stages, two strains decreased, and other strains of another side increased rapidly at the cracking loading, then they both rose until the plates failed.

KEYWORDS

Adhesive interface, CFRP, Steel plate, Shear stress, Experimental study

INTRODUCTION

As a new kind of reinforcing composite materials, CFRP has some advantages such as light weight, high strength and elasticity, easy construction, corrosion resistance, low thermal conductivity, electrical isolation, and has been used wildly in structural strengthening. The researches on the steel structural strengthening with CFRP are focus on bending reinforcement, tension reinforcement and fatigue reinforcement [1].

Narmashiri et al. investigated the failure modes of CFRP strengthened steel I-beams by four-points bending test and numerical simulation by ANSYS [2]. They found the failure modes depended on the specifications of CFRP plates. Siwowski and Siwowska compared the flexural behaviour of steel beams reinforced with CFRP in two strengthening schemes: adhesive-bonded passive plates and adhesive-bonded prestressed or active plates [3]. It found that the failure modes comprised CFRP plates debonding or plates rupture depending on the strengthening system and some system parameters. Colombi and Fava performed an experimental study on the fatigue property of cracked steel beams reinforced by CFR. The results shown that CFRP can reduce the fatigue crack growth and raise the fatigue life [4].

Sundarraja et al. made an experimental study and a numerical simulation on the axial CFRP-strengthened steel tubes with hollow square sections under compression load [5]. It concluded that the

increase in the CFRP strips thickness effectively delayed the local buckling of the tubes and led to the inward buckling rather than outward one. Niu and Jin made an analytical study on the buckling loading about the neutral axis with the maximum moments of inertia for a square steel tube with flange outsides wrapped by CFRPs based on Ježek method and considered an initial imperfection [6].

Some researches focus on the strengthening performance of steel structures with damage or cracks reinforced by CFRP. Hou et al. investigated the flexural behaviour of CFRP strengthened damaged steel beams by experimental study and finite element analysis [7]. Furthermore, they discussed the effect of prestress CFRP on the damaged steel beams [8]. Xie studied the capacities and interfacial crack propagation law of notched steel beams and notched steel plates strengthened with CFRPs by the finite element method [9]. In the finite element model, a mixed-mode cohesive law was employed to depict adhesive behaviour. Li and Li investigated the buckling performance of steel compression members with multiple local damages strengthened with CFRP under axial loading [10]. The elastic buckling load considered various boundary conditions was presented by using energy approach. Hu et al. proposes fatigue design guides and programs for CFRP-strengthened steel structures with initial cracks based on existing design codes and guidance for pure steel under fatigue loading [11]. Some typical design examples were given out for reference. Wang investigated the fatigue behaviour of central-cracked and double-edge-cracked steel structures strengthened with CFRPs by experimental study, numerical simulation and theorical method [12].

The authors' research group has been working on the strengthening technology of CFRP in engineering structures for over twenty years. The studies include the fatigue performance of reinforced concrete member strengthened with CFRP, strengthening technic of prestressed CFRP [13], fatigue crack propagation law of RC beams and steel plates with initial cracks strengthened with CFRP [14], and fatigue behaviour of the interface between CFRP and concrete beams under hygrothermal environment [15].

The adhesive interface is the weakest park of CFRP strengthened steel plates, in most cases, the debonding failure of the adhesive interface first occurs in the failure of the components [16-17]. Therefore, studying the mechanical properties of the adhesive interface is important to understand the overall mechanical properties of CFRP strengthened steel structures. This paper provides an experimental investigation on the shear performance of adhesive interface between CFRP and steel plates.

The remainder of the paper is organized as follows. Section 2 describes the experimental program in detail, including material properties, how specimens prepared, and experimental set-up and testing procedures. Experimental results are given out in Section 3. Failure characteristics are described, strain-loading curves are analyzed, and results discussion are presented in this section. The paper closes with brief conclusion in Section 4.

EXPERIMENTAL PROGRAMS

There are some experimental methods for bonding strength of steel structures strengthened with CFRP, such as simple shear model, twin shear model and beam type test. Comparing with simple shear model, twin shear model has simple and clear stress state and influenced few by normal stress. So, a twin shear model, as shown in Figure 1, is applied in this experiment to ensure the adhesive interface subjected to shear stress only.

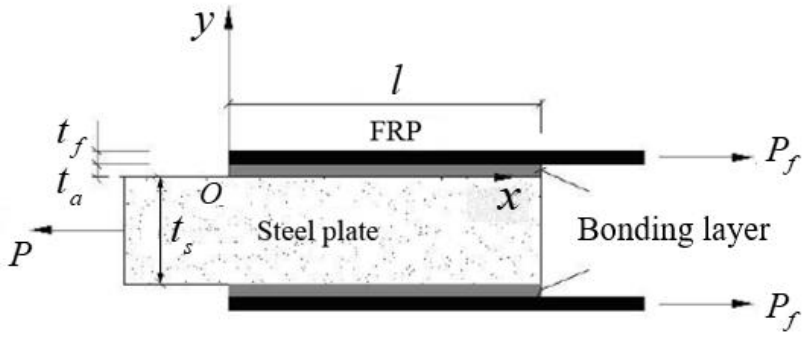

Fig. 1 - Twin shear model

Material properties

In this study, six steel plates strengthened with CFRPs are designed and tested under tensile loadings. The plates are made of Q345 No.10 I-steel, produced by Liuzhou Iron and Steel Company, with effective length of 200mm, width of 15mm, and nominal thickness of 3.5mm. Figure 2 shows the schematic of a steel plate. The mechanical properties of the steel, CFRP and adhesive are shown in Table 1. CFRP is used to strengthen the steel plates. The laminate has 200mm length, 15mm width, and 1.3mm calculating thickness. The carbon fiber silk is UT70-30, which is produced by Toray Company (Tokyo, Japan). Epoxy S-02 of Sikadur®-31SBA, produced by Sika Group, is used as adhesive for bonding the CFRP to the steel plates.

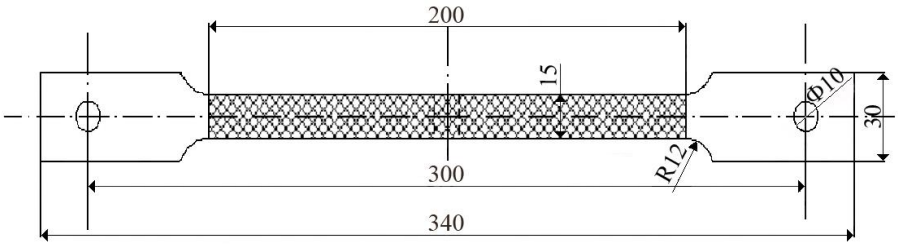

Fig. 2 - Schematic of a steel plate

Tab. 1 - Material properties of components

	Steel	CFRP	Adhesive
Tensile strength (MPa)	455	3780	
Yield strength (MPa)	345		
Shear strength (MPa)			15
Young's modulus (GPa)	206	230	5
Poisson's ratio	0.3	0.25	0.38
Thickness (mm)	3.5	1.3	1.0

Preparation of specimens

Two groups of steel plates with three specimens for each are prepared. The specimens in group A have a gap, with length 3.5mm, at the mid-span as shown in Figure 3. After being abrasive blasted, cleared by abrasive paper and acetone, the plates are bonded with CFRPs at both sides. The CFRPs should be blasted to increase the surface roughness, cleared by dry cloth to get rid of the

residue, cleaned by acetone, and then cut into size 200mm × 15mm, bonded to the plates by using the epoxy. The specimens in group B have no damage and bonded with CFRPs to compare with the specimens in group A. Resistance strain gages, with resistance 10ohms and sensitivity coefficient 2.0, are stick on the CFRPs. The stick locations are shown in Figure 4. For A-specimens, strains at the mid-span are tested and the gages are stick beside the gaps; for B-specimens, strains along CFRPs are considered and the gages are stick at the mid-span and two ends of CFRPs.

Fig. 3 - A steel plate with a gap at the mid-span

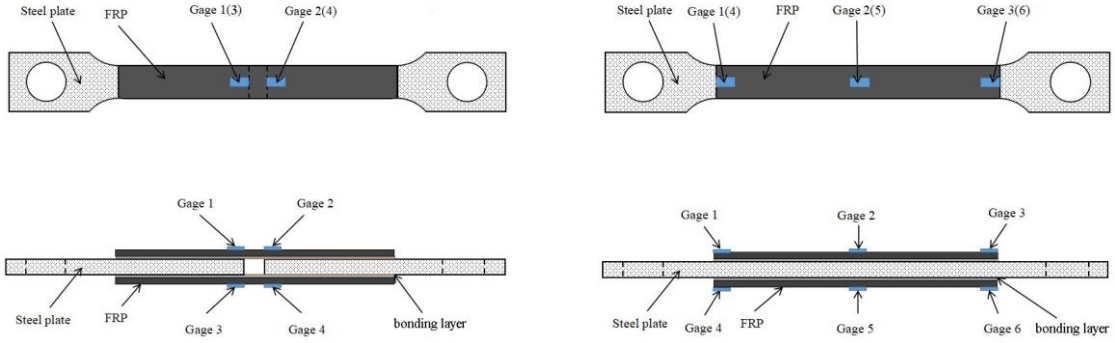

(a) *(b)*

Fig. 4 - Schematic of (a) steel plates with a gap, and (b) without damage bonded with CFRPs and strain gages

Experimental set-up and testing procedures

All the specimens are tested under tensile loadings by SANS's CMT5105 electronic universal testing machine. The machine has high testing precision and sensitivity in the measurement and control of loading, deformation and displacement, and is usually used to test metal specimens with loading under 100kN. The experimental equipment is shown in Figure 5. The strains of CFRPs are recorded by DataTaker's OM4B-DT85G Geologger data collecting system and TMR-7200 dynamic measurement software, as shown in Figure 6.

(a) (b)

Fig. 5 - (a) Testing machine and, (b) a specimen installed in the machine in (a)

Fig. 6 - Data Taker Geologger data collecting system

In this experiment, tension loadings are applied at the steel plates and the stresses transmit to the CFRPs via the adhesive interface. Shear stress appears at the interface between CFRP and steel plate and governs the specimens' failure. The details of testing procedure are listed as following:

(1) Install a specimen in the testing machine, check all the wires are connected correctly.

(2) Debug the data collecting system and let the initial strains be $\pm 4\mu\varepsilon$.

(3) Apply 5% of the maximum loading as initial loading to check if all the machines are working.

(4) Resume loading and control the loading speed at 0.5mm/min.

(5) Observe the CFRPs' debonding and the specimens' failure.

EXPERIMENTAL RESULTS AND DISCUSSION

Failure characteristics

For group A, the three specimens haven't obvious yield and shrinkage stages, and perform tensile behaviour of plastic materials without obvious yield stage. When the loading comes to a cracking loading, a crack appears at the end of the gap which cut through the bonding layer along 45° degree and expand along the interface between CFRP and bonding layer. The average cracking loading and crack strain of the cracked side are 14.85kN and 2728 $\mu\varepsilon$. After cracked, the strain of the cracked side would decrease rapidly and that of uncracked side would continue to increase. Finally, the specimens fail for CFRP debonding and the interface between steel and bonding layer are still undamaged. The cracking loadings and breaking loadings are listed in Table 2 and a failed specimen is shown in Figure 7(a).

Tab. 2 - Failure modes

Serial number	Cracking loading /kN	AVG Cracking loading /kN	Breaking loading /kN	AVG breaking loading /kN	Failure mode
A-1	14.93		--		Cracked at gap
A-2	14.76	14.85	17.81	17.88	Cracked at gap
A-3	14.85		17.96		Cracked at gap
B-1	--		21.50		Plate broken
B -2	--		21.45	21.47	Plate broken
B -3	--		21.48		Plate broken

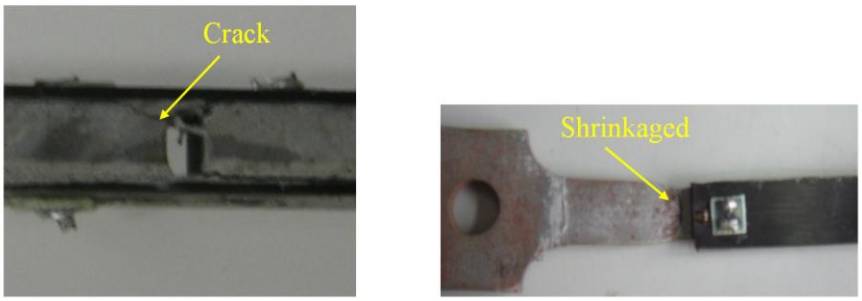

(a) *(b)*

Fig. 7 - (a) A specimen in group A failed for crack expanding, and (b) a specimen in group B failed for plate breaking

For group B, the three specimens perform tensile behaviour of plastic materials, i.e., the specimens go through four stages of elasticity, yield, reinforcement and shrinkage, and break at the end of CFRP. The bonding parts of CFRP and steel are undamaged. A broken specimen is shown in Figure 7(b). At the ends of CFRP, the steel plate has the minimum cross-section and they are possible failure parts. The maximum tension loading capacity of the steel plate is

$$F_{\max,t} = 455 \times (15 \times 3.5) = 21.5\text{kN} \quad (1)$$

The maximum shear loading the interface can bear is

$$F_{\max,s} = 15 \times (15 \times 100) = 22.5\text{kN} \quad (2)$$

The maximum tensile loading the CFRP can have is

$$F_{\max,FRP} = 3780 \times (15 \times 1.3) = 73.7\text{kN} \quad (3)$$

Because there are two adhesive interfaces and CFRPs bonded are two sides of plate, the possible loading for interface failure and CFRP break should be the double values in Eqs. (2) and (3). So, for the undamaged plates, they would fail for steel breaking. The breaking loadings are listed in Table 2 too.

Strain-loading curves

The strain gages stick on the plates in group B are all failed since the gages didn't stick firmly-cemented and deboned in the testing. The strain data of group B are unusable. This section will discuss the relationships between strain and loading for the plates in group A. Figure 8(a) shows the curves of strain-loading of plate A-1, where ε_1, ε_2, ε_3 and ε_4 denote the strain of gage 1, 2, 3 and 4, respectively. When the loading is less than 14.93kN, the curves are almost linear. When the loading comes 14.93kN, ε_1, ε_2 decrease rapidly, and ε_3, ε_4 increase fast. There is a crack appears at the interface between the steel and the bonding layer under gage 1 or 2, then it cut through the bonding layer and expand to the end of CFRP. The tensile stresses of CFRPs of the cracked side fall down, and the CFRP of another side sustains all the tensile loading which makes ε_3 and ε_4 increase. The machine stop loading at the time, and the specimen hasn't a breaking loading. Figure 8(b) is the displacement-loading curve of plate A-1. It shows that the deformation of steel plate is linear to the loading. Steel and CFRP have similar Young's modulus and the specimen is working in linear elastic stage. It can be concluded that the strains of plate are linear and close to that of CFRP.

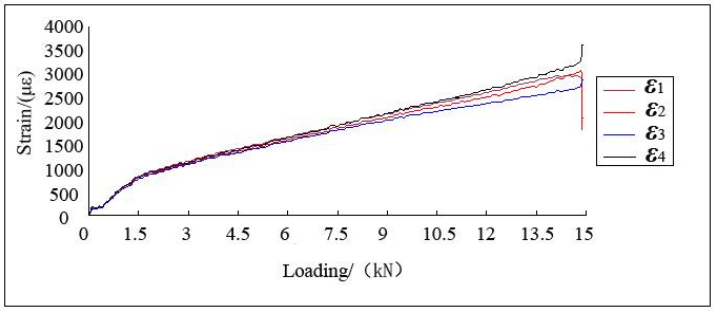

(a)

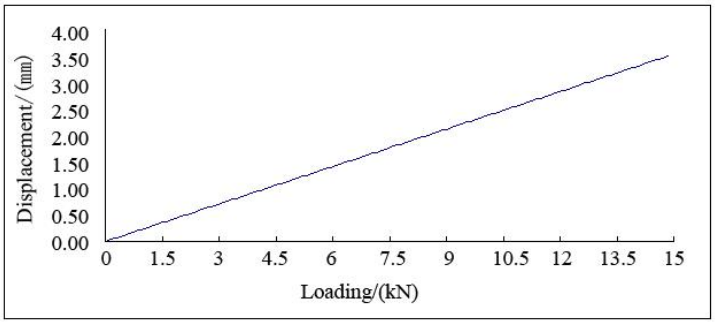

(b)

Fig. 8 - (a) Strain-loading curves and (b) displacement-loading curve of plate A-1

Figure 9 shows the strain-loading curves of plate A-2. When the loading is less than 14.76kN, the curves are almost linear. When the loading comes 14.76kN, ε_1 and ε_2 reduce 13% since a crack appears at the bonding layer of this side, and ε_3, ε_4 rise markedly. Then all the strains rise again when the loading increase but ε_3 and ε_4 are steeper. The specimen fails when the loading is 17.81kN and ε_3, ε_4 drop down to zero.

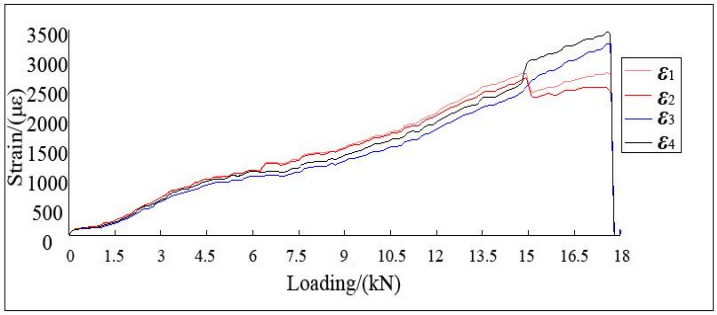

Fig. 9 - Strain-loading curves of plate A-2

For the loading applying is controlled by displacement, when the bonding layer of ε_1 and ε_2 side cracking, the deformation and length of the whole specimen doesn't change, but the length of unbonded CFRP increases which leads to the stiffness of this region decrease. So, ε_1 and ε_2, the strains of this region, decrease abruptly, and the CFRP of another side bears more stress which leads to ε_3, ε_4 increase. As the crack propagating, the strains increasing with the loading. The slopes of ε_1 and ε_2 become gentler, and that of ε_3 and ε_4 have no change.

Figure 10 shows the strain-loading curves of plate A-3. The cracking loading is 14.85kN. Like the curves of plate A-2, ε_1 and ε_2 reduce 15% and ε_3, ε_4 risen markedly when the loading comes to it, then all the strains increases again with the loading and the specimen fails when the loading is 17.96kN.

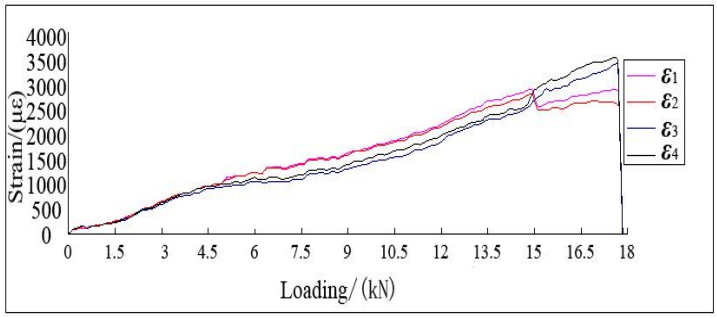

Fig. 10 - Strain-loading curves of plate A-3

The four strain gages in each specimen of group B are stick symmetrically and their values are supposed to be equal. In fact, the strains have differences in 5% at the same side and in 12% at different sides. The main reasons mainly lie in three aspects: 1) there are installation deviations of strain gages; 2) there are installation errors of specimens; 3) there are manufacturing deformations of specimens. The differences of gages lie in acceptable range, so the testing data are valid.

CONCLUSION

This paper provided an experimental investigation on the shear performance of adhesive interface between steel plate and CFRP. Six steel plates strengthened with CFRPs were prepared for the experiment, including three undamaged specimens and three with a gap. Twin shear model were applied in the test under tensile loadings. The experimental results showed that: (1) the undamaged plates broke for tensile failure, the CFRPs and the bonding layer were undamaged; (2) the plates with a gap failed for CFRPs debonding, a crack appeared at the end of the gap, cut through the bonding layer along 45° degree, and expanded along the interface between the CFRP and bonding layer; (3) the specimens with a gap cracked at 14.85kN and failed at 17.88kN; (4) the strain-loading curves had long linear stages, two strains decrease and other strains of another side increased rapidly at the cracking loading, then they both rose until the plates failed. This study will offer scientific basis and important consults to the strengthening design and research on steel structures reinforced by CFRP.

ACKNOWLEDGEMENT

This research was funded by the National Natural Science Foundation of China through Award (Nos. 12172134, 11872185) and the Natural Science Foundation of Guangdong Province through Award No. 2021A1515010037.

REFERENCES

[1] Teng, J.G., Yu, T., Fernando, D. (2012): Strengthening of steel structures with fiber reinforced polymer composites. *Journal of Constructional Steel Research*, vol. 78, pp. 131-143. *DOI:* 10.1016/j.jcsr.2012.06.011

[2] Narmashiri, K., Jumaat, M.Z., Sulong, N.H.R. (2011): Failure modes of CFRP flexural strengthened steel I-beams. *Key Engineering Materials*, vol. 471-472, pp. 590-595. *DOI:* 10.4028/www.scientific.net/KEM.471-472.590

[3] Siwowski, T.W., Siwowska, P. (2018): Experimental study on CFRP-strengthened steel beams. *Composites Part B: Engineering*, vol. 149, pp. 12-21. *DOI:* 10.1016/j.compositesb.2018.04.060

[4] Colombi, P., Fava, G. (2015): Experimental study on the fatigue behaviour of cracked steel beams repaired with CFRP plates. *Engineering Fracture Mechanics*, vol.145, pp. 128-142. *DOI*: 10.1016/j.engfracmech.2015.04.009

[5] Sundarraja, M.C., Sriram, P., Prabhu, G.G. (2014): Strengthening of hollow square sections under compression using FRP composites. *Advances in Materials Science & Engineering*, vol. 2014, pp. 1-19. *DOI:* 10.1155/2014/396597

[6] Niu, P., Jin, C.F. (2015): Analytical solutions on ultimate bearing capacity of a square CFRP-steel tube member with initial imperfection. *Engineering Mechanics,* vol. 32, no. s1, pp. 236-240. (in Chinese)

[7] Hou, W.Y., Wang, L.G. and Shi, D. (2022): Flexural behaviour of strengthened damaged steel beams using carbon fibre-reinforced polymer sheets. *Scientific Reports*, vol. 12, pp. 10342. *DOI*: 10.1038/s41598-022-14471-9

[8] Hou, W.Y., Wang, F.C. and Wang, L.G. (2021): Test and Numerical Analysis on Damaged Steel Beam Strengthened with Prestressed CFRP Sheet. *Advances in Civil Engineering*, vol. 2021, article ID: 6711877. *DOI*: 10.1155/2021/6711877

[9] Xie, Z.H. (2016): *Finite Element Analysis of interfacial stresses of cracked steel structures strengthened with CFRP plate*. Guangzhou: Guangdong University of Technology. (in Chinese)

[10] Li, B., Li, C.X. (2017): Investigation on the anti-buckling behavior of steel compression members with multiple local damage by FRP strengthening. *Industrial Construction*, vol. 47, no. 1, pp. 168-173. (in Chinese)

[11] Hu, L.L., Feng, P., Zhao, X.L. (2017): Fatigue design of CFRP strengthened steel members. *Thin-Walled Structures*, vol. 119, pp. 482-498. *DOI:* 10.1016/j.tws.2017.06.029

[12] Wang, H.T. (2016): *Study on the fatigue behavior of CFRP plate-strengthened steel structures and its design method*. Nanjing: Southeast University, 2016. (in Chinese)

[13] Guo, X.Y., Wang, Y.L., Huang, P.Y., Shu S.Y.H. (2020): Fatigue behavior of RC beams strengthened with FRP considering the influence of FRP-concrete interface. *International Journal of Fatigue*, vol. 143, pp. 105977. *DOI:* 10.1016/j.ijfatigue.2020.105977

[14] Yang, Y., Huang, C.H., Huang, P.Y. (2018): Surface crack propagation rules of CFL-strengthened steel plate under fatigue loading. *IOP Conference Series: Materials Science and Engineering*, vol. 392, no. 2, pp. 0220258. *DOI:* 10.1088/1757-899X/392/2/022028

[15] Chen, Z.B., Huang, P.Y., Guo, X.Y., Zheng, X.H., Yang, Y. (2020): Fatigue equation of structural materials and members under hot-wet environment and cyclic bending loads. *Strength, Fracture and Complexity*, vol. 12, no, 2-4, pp. 119-125. *DOI:* 10.3233/SFC-190241

[16] Jiang, X., Luo, C.W., Qiang, X.H., Kolstein, H., Bijilaar, F. (2017): Effects of Adhesive Connection on Composite Action between FRP Bridge Deck and Steel Girder. *Journal of Engineering*, vol. 2017, article ID: 6218949. *DOI*: 10.1155/2017/6218949

[17] Lozano, C.M., Riveros, G.A. (2019): Effects of Adhesive Bond-Slip Behavior on the Capacity of Innovative FRP Retrofits for Fatigue and Fracture Repair of Hydraulic Steel Structures. *Materials*, vol. 12, no. 9, pp. 1495. *DOI*: 10.3390/ma12091495